

Mixing and Coherent Structures in Two and Three Dimensional Containers

Tatyana S. Krasnopolskaya¹, Volodymyr S. Malyuga¹ and Oleksandr L. Golichenko²

¹ Institute of Hydromechanics NASU, 03680 Kiev, Ukraine
(E-mail: t.krasnopolskaya@tue.nl; v_s_malyuga@ukr.net)

² Kiev National Taras Shevchenko University, Kiev, Ukraine
(E-mail: Golichenko_O_L@mail.ru)

Abstract. This study addresses problems: what determines coherent structures in mixing patterns and what are main elements of the coherent structures. We restrict our consideration to finite times and are mainly interested in how to organize steady or periodic flow and where to put the blob (or blobs) in order to achieve the best result in that finite time. Knowing types and positions of periodic points coherent structures in distributive mixing patterns could be classified. These structures are connected with hyperbolic and elliptic periodic points and lines for three-dimensional mixing flows.

Keywords: Distributive mixing, Periodic points and lines, Coherent structures.

1 Introduction

We consider the laminar mixing process in a two-dimensional annular wedge-shaped cavity and in a three-dimensional creeping flow of a viscous incompressible fluid contained in a finite circular cylinder, induced by a prescribed periodic motion of the end walls. Here we apply a method to locate periodic structures and manifolds. In contrast to two-dimensional flow of an incompressible fluid, for which the equations of motion of an individual passive particle can always be written in Hamiltonian form and for which well-developed methods of Hamiltonian mechanics can be applied, the study of three-dimensional mixing flows encounters considerable difficulties. An important characteristic of both two-dimensional and three-dimensional flows, that is closely related to the problem of determination of the regions of regular behaviour being barriers for the mixing process (Aref[1]), is the location of periodic points (or fixed points in the hyperplane of the Poincaré map). The determination and classification of periodic points in three-dimensional flows is a complicated problem. Furthermore, in three-dimensional flows these points can form one-dimensional periodic lines. A complete classification of the periodic points can be performed in accordance

Received: 30 March 2013 / Accepted: 12 July 2013

© 2013 CMSIM



ISSN 2241-0503

with three eigenvalues of the linearized matrix of the Poincaré map, and specific behaviour of the map near such a point can be associated with its type [4]. Generally, the periodic points of three-dimensional flows could be characterized by a much richer variety, compared to the points of two-dimensional flows, in which only three possible types exist. However, if in a three-dimensional flow the point lies on a periodic line it is not significantly different from periodic points in two-dimensional flows. In the three-dimensional case, the flow near a periodic line is topologically similar to the flow near a periodic point in two-dimensional case.

2 Stirring of a viscous incompressible fluid

2.1 Mixing in a two-dimensional annular wedge-shaped cavity

As a first example of mixing, we consider a two-dimensional creeping flow of an incompressible viscous fluid in an annular wedge cavity, $a \leq r \leq b$, $|\theta| \leq \theta_0$, driven by periodically time-dependent tangential velocities $V_{bot}(t)$ and $V_{top}(t)$ at the curved bottom and top boundaries, when a radius r is $r = a$ and $r = b$, respectively. The side walls, $a \leq r \leq b$, $|\theta| = \theta_0$ are fixed. We consider a discontinuous mixing protocol with the bottom and top walls alternately rotating over an angle Θ in clockwise and counterclockwise directions, respectively. More specifically, we consider the case

$$\begin{aligned} V_{bot}(t) &= \frac{2a\Theta}{T}, V_{top}(t) = 0, \quad \text{for } kT < t \leq \left(k + \frac{1}{2}\right)T, \\ V_{bot}(t) &= 0, \quad V_{top}(t) = -\frac{2b\Theta}{T}, \\ &\text{for } \left(k + \frac{1}{2}\right)T < t \leq (k+1)T, \end{aligned} \quad (1)$$

where $k = 0, 1, 2, \dots$. Θ is the angle of wall rotation and T is the period of the walls motion. The radial and azimuthal velocity components u_r and u_θ can be expressed by means of the stream function $\Psi(r, \theta, t)$ as

$$u_r = \frac{1}{r} \frac{\partial \Psi}{\partial \theta}, \quad u_\theta = -\frac{\partial \Psi}{\partial r}. \quad (2)$$

For a quasi-stationary creeping flow in the Stokes approximation the stream function Ψ satisfies the biharmonic equation

$$\nabla^2 \nabla^2 \Psi = 0, \quad (3)$$

with the Laplace operator ∇^2 and the boundary conditions

$$\Psi = 0, \quad \frac{\partial \Psi}{\partial r} = -V_{bot}, \quad \text{at } r = a, \quad |\theta| \leq \theta_0, \quad (4)$$

$$\Psi = 0, \quad \frac{\partial \Psi}{\partial r} = -V_{top}, \quad \text{at } r = b, \quad |\theta| \leq \theta_0, \quad (5)$$

$$\Psi = 0, \quad \frac{\partial \Psi}{\partial \theta} = 0, \quad \text{at } a \leq r \leq b, \quad |\theta| = \theta_0. \quad (6)$$

Therefore, we have the classical biharmonic problem for the stream function Ψ with prescribed values of this function and its outward normal derivative at the boundary.

The system of ordinary differential equations

$$\frac{dr}{dt} = \frac{1}{r} \frac{\partial \Psi}{\partial \theta}, \quad r \frac{d\theta}{dt} = -\frac{\partial \Psi}{\partial r} \quad (7)$$

with the initial conditions $r = r_{in}$, $\theta = \theta_{in}$ at $t = 0$ describes the motion of an individual (Lagrangian) particle occupying the position (r, θ) at time t . In fact, we have steady motion of the particle within time intervals $(kT, kT + T/2)$, $(kT + T/2, kT + T)$, with velocities that instantaneously change at $t_k = kT/2$, $(k = 0, 1, 2, \dots)$.

It is easy to check that, within these intervals, when the stream function does not explicitly depend on time, system (11) has the first integral $\Psi(r, \theta) = \text{const}$. Therefore, this system is integrable and a particle initially at (r_{in}, θ_{in}) moves along a steady streamline during the first half period $(0, T/2)$. At the instant $t = T/2$ when the forcing is switched, the topology of streamlines is changed, and the particle instantaneously moves along a new streamline during the second half of period $(T/2, T)$, and so on. The spatial position of the particle is continuous, but its velocity experiences a discontinuity at each half period.

It is because of these abrupt periodical changes in the velocity field that the question of stability and instability of the solution of system (11) and possibility of chaotic advection (Aref[1]) naturally arises.

The problem of mixing of a certain amount of dyed passive material (the blob), as considered here, consists of tracking in time the positions of particles initially occupying the contour of the blob, say, the circle of radius R with the center at (r_c, θ_c) . We assume that the flow provides only a continuous transformation of the initially simply connected blob. Therefore, the deformed contour of the blob gives the whole picture of the mixing.

This wedge-cavity flow problem has been solved analytically by Krasnopol'skaya *et al.*[2]. Their analytical solution was used for the numerical evolution of the interface line between the marker fluid and the ambient fluid, which was carried out by the dynamical contour tracking algorithm.

2.2 Statement of mixing problem in a cylinder

Consider the three-dimensional Stokes flow in a finite cylinder that occupies the domain $0 \leq r \leq a$, $0 \leq \theta \leq 2\pi$, $0 \leq z \leq H$ in the cylindrical coordinates (r, θ, z) . In terms of the velocity vector \mathbf{u} and the pressure p , the Stokes flow of an incompressible viscous fluid (inertia terms being negligible) is governed by

$$\mu \nabla^2 \mathbf{u} = \nabla p, \quad \nabla \cdot \mathbf{u} = 0, \quad (8)$$

where ∇ , $\nabla \cdot$, and ∇^2 stand for standard differential operations of gradient, divergence, and the Laplacian operator, respectively, and μ is the coefficient

of shear viscosity of the fluid. The flow is generated by periodic motion of the cylinder end wall at $z = H$, while the cylinder wall $r = a$ remains fixed. In terms of Cartesian components, with the positive x -axis coinciding with the direction $\theta = 0$, the velocity vector $\mathbf{u} = u \mathbf{e}_x + v \mathbf{e}_y + w \mathbf{e}_z$ takes the following form at the domain boundaries:

$$\mathbf{u} = u_{top}(t) \mathbf{e}_x + v_{top}(t) \mathbf{e}_y, \quad z = H, \quad 0 \leq r \leq a, \quad 0 \leq \theta \leq 2\pi, \quad (9)$$

In what follows we consider one typical protocol of the wall motions with a constant velocity V and with period T (only the non-zero velocities are presented below). Protocol consists of two ‘zigzag’ steps of the top wall only:

$$u_{top} = V, \quad 0 \leq t \leq \frac{1}{2}T, \quad v_{top} = V, \quad \frac{1}{2}T \leq t \leq T. \quad (10)$$

Note that the protocol is discontinuous, although the motion of the fluid inside the cylinder is steady at any time within the whole period. Since the inertia forces are neglected in the governing equations (8), these steady motions are established instantaneously. Because of the linearity of system (8) and the absence of time dependent terms, the velocity field in the cylinder is periodic with period T .

Important for further analysis is the dimensionless kinematic parameter $D = VT/a$, which represents the ratio of two typical time scales of any given protocol: the forcing period T and the advection time a/V (for a wall travelling over a typical distance a with a velocity V).

The mixing process taking place is due to advection of passive material tracers by the velocity field \mathbf{u} and is hence governed by the three-dimensional system of ordinary differential equations

$$\frac{dx}{dt} = u(x, y, z, t), \quad \frac{dy}{dt} = v(x, y, z, t), \quad \frac{dz}{dt} = w(x, y, z, t), \quad (11)$$

with initial conditions $x = x_0, y = y_0, z = z_0$ at $t = 0$.

A full analytical solution for the linear vector boundary problem for the velocity field has been constructed by Meleshko *et al.*[5]. by the method of superposition. The principal idea of the method consists in representing the velocity field in the finite cylinder as the sum of two velocity fields: one for an infinite layer with thickness equal to the finite cylinder height, and another for an infinite cylinder with a radius equal to that of the original cylinder. Velocities in these simple domains are represented in the form of ordinary Fourier series with sets of arbitrary coefficients on the complete systems of Bessel and trigonometric functions, respectively. These series both identically satisfy the governing equation inside the domain and have sufficient functional arbitrariness for fulfilling any boundary conditions on the top and bottom walls and on the lateral surface of the cylinder, respectively. Because of the interdependency, the expression for a coefficient of a term in one series will depend on all the coefficients of the other series and vice versa. The final solution involves solving an infinite system of linear algebraic equations, providing the relations between applied velocities and the coefficients in two ordinary Fourier series

on the complete systems of Bessel and trigonometric functions in radial and axial directions, respectively. The general theory of such infinite systems provides leading terms in the asymptotic behaviour of coefficients. An established technique was used to considerably improve the convergence of the series on the whole boundary, including the rims. The numerical results presented in Meleshko *et al.*[5] reveal that the boundary conditions for the case of a lid-driven cavity are satisfied within the accuracy $\mathcal{O}(10^{-3})$ in comparison with the prescribed velocity, even at the corner point.

The problem of accurate determination of the interface is obviously very complicated, as it moves and deforms with the flow. There exist many techniques to deal with flows containing sharp fronts, which can be divided into two basic strategies – front-capturing and front-tracking. Detailed reviews of the front-tracking methods are provided by Krasnopolskaya *et al.*[3] and Malyuga *et al.*[4].

2.3 Periodic points and lines

A periodic point \mathbf{P} of period n can be classified as an elliptic, hyperbolic, or parabolic point depending upon the structure of the surrounding flow field. This classification is based on the behaviour (in the course of time) of an infinitesimally close neighbouring point $\mathbf{P} + d\mathbf{x}_0$. After n periods, the latter arrives at $\mathbf{P} + d\mathbf{x}_n = \Phi_T^n(\mathbf{P} + d\mathbf{x}_0)$, upon linearization about the periodic point $\mathbf{P} = \Phi_T^n(\mathbf{P})$, adding up to

$$d\mathbf{x}_n = F \cdot d\mathbf{x}_0 \tag{12}$$

with $F = \partial\Phi_T^n/\partial\mathbf{x}|_{\mathbf{P}}$ the real Jacobian matrix. According to (12), stable and unstable structures may emerge, depending on the properties of the matrix F . In order to analyse the nature of the map near \mathbf{P} , the relation (12) is rewritten in the canonical (or Jordan) form

$$\boldsymbol{\eta}_n = S \cdot \boldsymbol{\eta}_0 \quad S = R^{-1} \cdot F \cdot R \quad \boldsymbol{\eta} = R^{-1} \cdot d\mathbf{x} \tag{13}$$

with R the transformation matrix relating the local Cartesian (dx, dy, dz) to the canonical $(\eta^{(1)}, \eta^{(2)}, \eta^{(3)})$ frame of reference.

In two-dimensional systems, elliptic points are surrounded by islands, sealing off the elliptic region from the remainder of the flow domain and in consequence acting as transport barriers. The hyperbolic points \mathbf{x}_h are accompanied by stable manifolds $W^s(\mathbf{x}_h)$ and unstable manifolds $W^u(\mathbf{x}_h)$ that merge either into closed orbits or display transversal intersection. The former phenomenon is reminiscent of the aforementioned elliptic islands by obstructing communication between flow regions, whereas the latter brings about excessive stretching and folding of material elements, indicative of chaotic advection [1]. In the three-dimensional domain of interest the islands and manifolds, associated with periodic points on the elliptic and hyperbolic segments of the periodic line, readily merge into tubular objects and intricate surfaces, although possessing essentially two-dimensional characteristics.

The periodic lines of period-2 of the flow generated in a cylinder are shown in figure 1

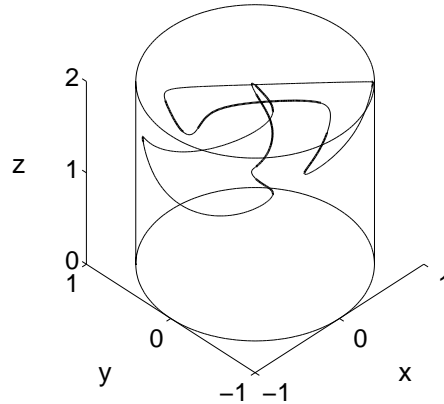


Fig. 1. The periodic lines of period-2 in the flow in the cylinder for $D = 5$. Thick and thin lines represent the elliptic and hyperbolic segments, respectively [4].

Such lines were found to exist only for $D > 2$. It is worth noting that each of the two lines returns into itself after two periods. Although any periodic point of second order exists always in combination with another one, they can belong to the same periodic line of the second order.

3 Coherent structures

The results presented correspond to one typical wedge cavity with $\theta_0 = \pi/4$ and $b/a = 2$. Using the dimensionless parameter $H = \Theta/\theta_0$ and a fixed value for the period T , the discontinuous mixing protocol (1) is completely defined. We restrict our consideration to the case $H = 4$. The accurate Lagrangian description of the contour line provides the possibility to construct an Eulerian representation of the mixture. Figure 2(a) shows the mixed state with the positions of the initially circular blob (green area) after six periods (red) and after twelve periods (blue). There are two main components of the coherent structure in the mixed state: one component formed by the thin filaments with their striation decreasing in time and the other one by the small ‘rubbery’ region, representing the unmixed part of the blob. What creates this structure? First of all, the invariant unstable manifold corresponding to the hyperbolic point of period-1 which is located in the centre of the original green blob (indicated by a black square in the middle in figure 2b). This manifold, presented in the figure 3(a), serves as a skeleton which forms the first main coherent structures of the deforming blob. The origin of the ‘rubbery’ coherent structure can be explained in terms of the existence of elliptic periodic points of period-6, period-2 and period-6, respectively, which are shown as white boxes in figure 2(b). In the upper part of the green circular blob (figure 2b), a small black box indicates the position of the hyperbolic fixed point of period-6 and therefore, the ‘rubbery’ region nearby this point will be destroyed completely in course of time.

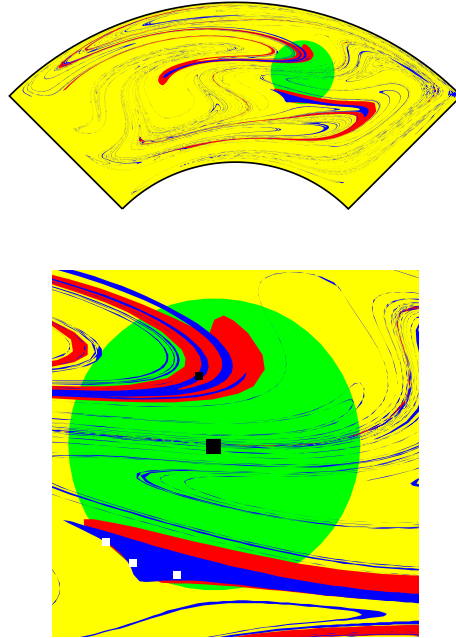


Fig. 2. Mixing patterns: (a) in the whole cavity; (b) in the region of the initial blob position.

The resulting deformation after twelve periods of small circular domains surrounding these higher order periodic points are shown in figure 3(b). The small circular blob surrounding the hyperbolic point transforms after twelve periods into a thin red line, while the three circular bolbs surrounding the elliptic points only slightly deform (the so-called ‘rubbery’ regions).

4 Conclusions

Coherent structures in distributive mixing patterns are classified. These structures are connected with hyperbolic and elliptic periodic points (and lines) of order-1 or higher.

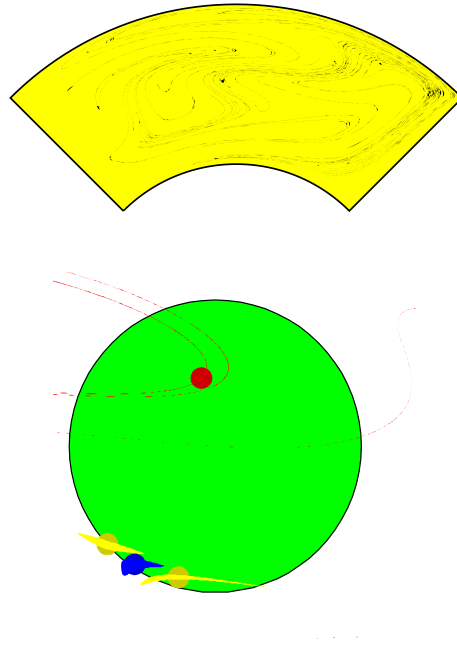


Fig. 3. The elements of coherent structures: (a) part of unstable manifold of the hyperbolic point of period-1 in the centre of the initial blob; (b) deformation patterns of small circular blobs surrounding periodic points of higher order.

References

1. H. Aref. Stirring by chaotic advection. *J. Fluid Mech.* 143: 1–24, 1984.
2. T. S. Krasnopolskaya, V. V. Meleshko, G. W. M. Peters and H. E. H. Meijer. Steady Stokes flow in an annular cavity. *Q. J. Mech. Appl. Math.*, 49: 593–619, 1996.
3. T. S. Krasnopolskaya, V. V. Meleshko, G. W. M. Peters and H. E. H. Meijer. Mixing in Stokes flow in an annular wedge cavity. *Eur. J. Mech. B/Fluids*, 18: 793–822, 1999.
4. V. S. Malyuga, V. V. Meleshko, M. F. M. Speetjens, H. J. H. Clercx and G. J. F. van Heijst. Mixing in the Stokes flow in a cylindrical container. *Proc. R. Soc. London, A* 458: 1867–1885, 2002.

- 5.V. V. Meleshko, V. S. Malyuga and A. M. Gomilko. Steady Stokes flow in a finite cylinder. *Proc. R. Soc. London, A* 456: 1741–1758, 2000.